

ENHANCED, HIGH RESOLUTION RADAR IMAGING BASED ON ROBUST REGULARIZATION

Müjdat Çetin and W. Clem Karl

Multi-Dimensional Signal Processing Laboratory, Dept. of ECE
Boston University, 8 Saint Mary's Street, Boston, MA 02215, USA

ABSTRACT

We propose an enhanced image reconstruction method for spotlight-mode synthetic aperture radar (SAR). Our approach involves extension of feature preserving regularization techniques developed in other applications to the complex-valued SAR imaging problem. Compared to conventional image formation schemes, our approach offers increased resolvability of point-scatterers, enhancement of object shapes, reduced sidelobes and reduced speckle. We present the effectiveness of the proposed method on synthetic and real SAR scenes.

1. INTRODUCTION

SAR is a microwave sensor capable of producing high resolution images of the earth's surface. A SAR system sends electromagnetic pulses from a radar mounted on an airborne or spaceborne platform to a particular area of interest on the ground and records the return signals. In order to achieve high cross-range resolution, SAR collects data from multiple observation points, and focuses the received information coherently to reconstruct a high-resolution 2-D description of the scene. The reflectivities of the underlying field in SAR are in general modeled to be complex-valued. This captures both amplitude scaling and phase shifting of the transmitted waveform by the scatterers. For most SAR scenes the phase of the reflectivity at a certain location can be modeled to be random, and uncorrelated with the phase at other locations [1].

In this paper, we will consider a particular type of SAR, called spotlight-mode SAR. A typical observation geometry for spotlight-mode SAR is shown in Figure 1. The mathematical relationship between the underlying field to be imaged, and spotlight-mode SAR observations (after demodulation) can be approximately expressed by a band-limited, offset-frequency Fourier

transformation [1, 2]. The data, hence the known samples of the Fourier transform of the field, lie on a polar grid in the spatial frequency domain.

The standard image formation algorithm used in essentially all SAR systems today is the polar format algorithm [1, 2] based on the two-dimensional fast Fourier transform (FFT). In this method, the data samples are first interpolated to a Cartesian grid, and then an inverse 2-D FFT is employed for image formation.

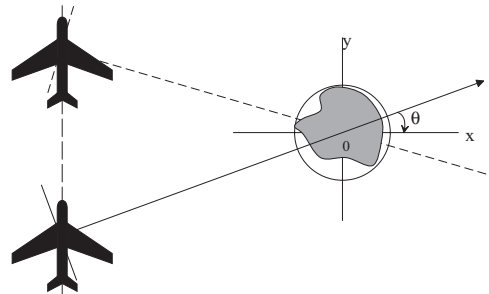


Figure 1: Ground-plane geometry for data collection in spotlight-mode SAR.

There are two important shortcomings of this approach. First, the achievable resolution is limited by the available system bandwidth. Second, the method does not allow the inclusion of prior information or constraints about either the data quality or the underlying reflectivity function, making the reconstruction sensitive to incomplete or noisy measurements.

There has recently been attempts to design alternative methods for SAR image formation. Of particular interest are the spectral estimation-based methods [3–5] and the entropy-based methods [6–9]. Spectral estimation-based methods have been shown to be quite successful in preserving gain on ideal point scatterers and in increasing the resolution beyond the Fourier limit. However, most spectral estimation-based methods reduce gain on non-pointlike scatterers such as trees, hence they fail to improve the quality of images containing objects with distributed features. The other

This work was supported by the Air Force Office of Scientific Research under Grant F49620-96-1-0028, the National Institutes of Health under Grant NINDS 1 R01 NS34189, and the Army Research Office under Grant ARO DAAG55-97-1-0013.

class of recent methods, the so-called entropy-based methods have been shown to offer good noise suppression properties. The experimental results in published work however, are too limited to show other possible advantages over conventional methods. Rather than realistic SAR scenes, most results involve examples which are simplified either in terms of the scene composition, or in terms of the complex-valued nature of the reflectivities.

Our objective is to devise a method which is useful under realistic assumptions for SAR and which has the ability to preserve features of both point scatterers and distributed objects. To attain this goal, we propose a model-based, regularized inversion scheme. Our method can be seen as an extension of feature-preserving regularization schemes developed in real-valued image processing [10, 11] to the SAR problem. Unlike these standard regularization problems, SAR involves *complex-valued* reflectivities. This has been a stumbling block for many methods proposed for SAR, but our approach effectively incorporates this property.

Although our development is primarily for SAR, the method can be extended to other domains involving complex signals such as holography and radio astronomy.

2. OBSERVATION MODEL

We assume data are collected by a radar traversing a flight path as in Figure 1. At multiple locations of the aircraft, high-bandwidth pulses¹ are transmitted and returns from the ground patch are then received and processed. After demodulation, the measurements obtained at observation angle θ can be written as:

$$r_\theta(\Omega) \approx F(\Omega \cos \theta, \Omega \sin \theta) \quad (1)$$

where Ω is the spatial frequency in the radial direction and $F(\cdot, \cdot)$ denotes the 2-D Fourier transform of the field $f(x, y)$ on a polar grid, whose location and extent in the frequency plane are determined by system parameters. The relationship in (1) can also be viewed as a tomographic one [12]. After combining the data from all observation angles, and discretization, we can obtain the following observation model [13]:

$$g = Tf + w \quad (2)$$

where w accounts for additive measurement noise, g is the full set of sampled data column stacked as a vector, T is a complex-valued matrix representing the tomographic, discrete SAR forward model, and f is the sampled field to be imaged, column stacked as a vector.

¹The most common signals used are linear FM chirp signals, which we will assume here.

3. IMAGE FORMATION SCHEME

3.1. Overview

We will formulate the image reconstruction problem as an optimization problem of the following form:

$$\hat{f} = \arg \min_f [\|g - Tf\|_2^2 + \lambda_1^2 \|f\|_1 + \lambda_2^2 \|D|f|\|_1] \quad (3)$$

where $\|\cdot\|_1$ and $\|\cdot\|_2$ denote the ℓ_1 and ℓ_2 norms respectively, and D is a 2-D derivative operator. The first term in the above objective function is a data fidelity term. The other two terms reflect the prior information we would like to impose.

Use of prior constraints based on ℓ_1 rather than ℓ_2 norms has recently become popular e.g. in image restoration [10], due to the ability of these constraints to prevent suppression of useful features in the image. The objective function in (3) extends the use of such constraints to the complex-valued SAR image reconstruction problem.

Since SAR object recognition methods usually rely on dominant point scatterer locations and/or object shapes, we use an explicit prior term in (3) for each type of feature. The term $\|f\|_1$ is an energy-type constraint on the solution, and aims to suppress artifacts and increase the resolvability of point scatterers. The $\|D|f|\|_1$ term on the other hand, imposes piecewise smoothness on the reflectivity magnitudes of the field. Using $\|Df\|_1$ as in real-valued image restoration would not be very useful for the complex-valued, random-phase SAR images, since this would penalize the real and imaginary parts of the reflectivities, and might not necessarily produce the desired piecewise smoothing for the magnitude images. Note that the additional level of non-linearity introduced by $D|f|$ creates a more challenging optimization problem than that based on Df . The relative magnitudes of λ_1 and λ_2 determine the emphasis on point-based versus shape-based properties.

3.2. Algorithm

In order to avoid problems due to non-differentiability of the ℓ_1 norm around the origin, we will use a smooth approximation to the ℓ_1 norm as in [10]. This leads to the following modified cost function:

$$\|g - Tf\|_2^2 + \lambda_1^2 \sum_{i=1}^N \sqrt{|(f)_i|^2 + \beta} + \lambda_2^2 \sum_{i=1}^M \sqrt{|(D|f|)_i|^2 + \beta} \quad (4)$$

where $\beta \geq 0$ is a constant, N and M are the lengths of the associated vectors, and $(\cdot)_i$ denotes the i th vector element. This optimization problem does not have

a closed-form solution in general. The numerical solution we propose is a specific quasi-Newton method. In particular, we will use a Hessian approximation $\tilde{H}(f)$ which is based on a quadratic approximation, and can effectively deal with both the complex nature of f , and the non-linearity associated with $D|f|$:

$$\tilde{H}(f) = 2T_b^T T_b + \lambda_1^2 Q_1(f) + \lambda_2^2 Q_2(f) \quad (5)$$

where

$$Q_1(f) = \begin{bmatrix} \Lambda_1(f) & 0 \\ 0 & \Lambda_1(f) \end{bmatrix} \quad (6)$$

$$\Lambda_1(f) = \text{diag} \left\{ \frac{1}{\sqrt{|(f)_i|^2 + \beta}} \right\} \quad (7)$$

$$Q_2(f) = \Phi^T(f) \begin{bmatrix} D^T \Lambda_2(f) D & 0 \\ 0 & D^T \Lambda_2(f) D \end{bmatrix} \Phi(f) \quad (8)$$

$$\Phi(f) = \begin{bmatrix} \text{diag} \{ \cos(\phi[(f)_i]) \} & \text{diag} \{ \sin(\phi[(f)_i]) \} \\ \text{diag} \{ -\sin(\phi[(f)_i]) \} & \text{diag} \{ \cos(\phi[(f)_i]) \} \end{bmatrix} \quad (9)$$

$$\Lambda_2(f) = \text{diag} \left\{ \frac{1}{\sqrt{|(D|f)|_i|^2 + \beta}} \right\} \quad (10)$$

$$T_b = \begin{bmatrix} \Re(T) & -\Im(T) \\ \Im(T) & \Re(T) \end{bmatrix}. \quad (11)$$

Here $\phi[(f)_i]$ denotes the phase of the complex number $(f)_i$, $\text{diag}\{\cdot\}$ is a diagonal matrix whose i th diagonal element is given by the expression inside the brackets, and $\Re(\cdot)$ and $\Im(\cdot)$ denote the real and imaginary components respectively.

Defining $\xi_b = [\Re(\xi)^T \Im(\xi)^T]^T$ with $\xi = \{f, g\}$, we obtain the following iteration, which we start with an initial vector $\hat{f}_b^{(0)}$, and run until convergence is achieved:

$$\hat{f}_b^{(n+1)} = (1 - \alpha) \hat{f}_b^{(n)} + \alpha \left(\tilde{H}(\hat{f}_b^{(n)}) \right)^{-1} 2T_b^T g_b \quad (12)$$

where α is the step-size. We terminate the iteration whenever $\frac{\|\hat{f}_b^{(n+1)} - \hat{f}_b^{(n)}\|_2}{\|\hat{f}_b^{(n)}\|_2} < \epsilon$, where ϵ is a small positive constant. Compared to standard optimization tools, this yields a quite efficient numerical scheme.

4. EXPERIMENTAL RESULTS

First, we will demonstrate the effectiveness of our method in enhancing point-based features. For this task, we set $\lambda_2 = 0$ in (4). Figure 2(a) shows the contour plot of a simple synthetic scene composed of eight point scatterers with unit reflectivity magnitudes. The bandwidth of the simulated SAR system in this case is not sufficient for resolving all the scatterers, which is apparent from the conventional reconstruction shown in

Figure 2(b). On the other hand, our method is able to resolve all scatterers as illustrated in Figure 2(c). Figure 3 shows the conventional SAR image and our result for a scene containing a military target. Our method produces an image in which dominant scatterers are enhanced, and sidelobes are considerably suppressed.

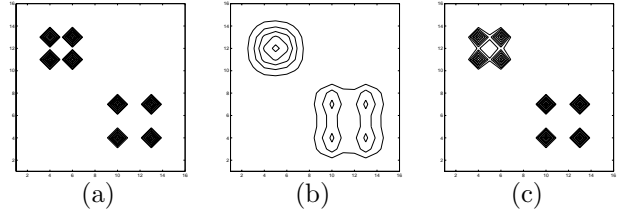


Figure 2: Reconstructions of synthetic point reflectors. (a) Truth (b) Conventional method (c) Proposed method.

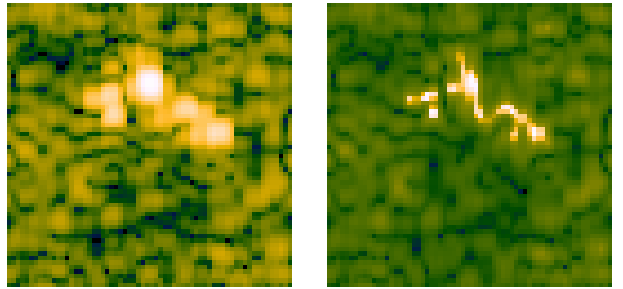


Figure 3: Left: Conventional SAR image of a military vehicle. Right: Superresolution reconstruction with the proposed method.

Next we will consider preserving region-based features. For this task, the dominant prior information term in (4) should naturally be the one based on $\|D|f|\|_1$. However we do not set λ_1 to 0, since we have empirically determined that some energy constraint helps in preserving the shadow in most SAR scenes. Figure 4 contains the reconstructions obtained by the conventional method and our approach for a scene with a military target. Our method provides smoothness in homogeneous regions without destroying the edges and general shape of the object. In addition to its visual appeal, this kind of an image would be preferred by automatic target recognition algorithms, since it can be segmented very easily into regions.

Finally, in Figure 5, we present the reconstructed images for a natural scene consisting of trees, two corner reflectors, plain fields and a road. Our method forms an image in which the tree shapes and shadows are very distinguishable, and the background is quite smooth, whereas the conventional SAR image suffers from considerable amount of speckle.

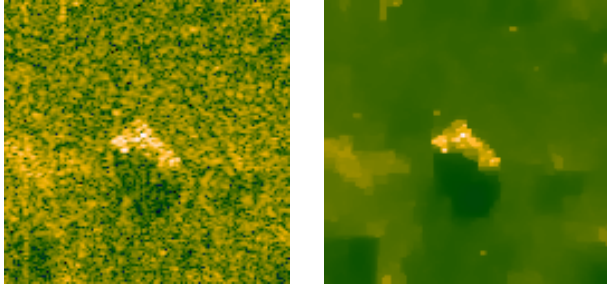


Figure 4: Left: Conventional SAR image of a military vehicle. Right: Reconstruction with shape-based feature preservation.

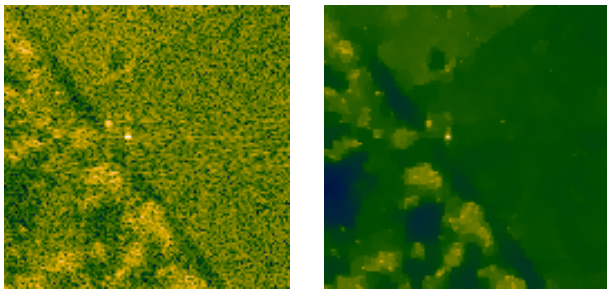


Figure 5: Left: Conventional SAR image of a natural scene. Right: Reconstruction with shape-based feature preservation.

5. CONCLUSIONS

We have proposed and demonstrated the viability of a regularized image formation method for complex-valued SAR imaging, using ℓ_1 -norm-based prior constraints to preserve two types of critical features. Our approach is a promising alternative to standard methods especially in applications where an automated decision making is to follow image reconstruction. Our current research involves quantitative assessment of potential performance improvements our method can provide for segmentation/recognition processing, and extension of our method towards a variational framework.

6. REFERENCES

- [1] C. V. Jakowatz Jr., D. E. Wahl, P. H. Eichel, D. C. Ghiglia and P. A. Thompson, *Spotlight-mode Synthetic Aperture Radar: a Signal Processing Approach*. Boston: Kluwer Academic Publishers, 1996.
- [2] W. G. Carrara, R. S. Goodman, and R. M. Majewski, *Spotlight Synthetic Aperture Radar: Signal Processing Algorithms*, Boston: Artech House, 1995.
- [3] S. R. Degraaf, "SAR imaging via modern 2-D spectral estimation methods," *IEEE Trans. Image Processing*, vol. 7, no. 5, pp. 729-761, May 1998.
- [4] J. Li and P. Stoica, "An adaptive filtering approach to spectral estimation and SAR imaging," *IEEE Trans. Signal Processing*, vol. 44, no. 6, pp. 1469-1484, June 1996.
- [5] G. R. Benitz, "High-definition vector imaging," *Lincoln Laboratory Journal*, vol. 10, no. 2, pp. 147-170, 1997.
- [6] B. Borden, "Cross-entropy regularization and complex-valued image analysis applicable to ISAR," *Proceedings of the SPIE Conference on Radar Processing, Technology, and Applications*, pp. 175-182, Aug. 1996.
- [7] B. R. Frieden and A. T. Bajkova, "Entropic reconstruction of complex images," *Optics Communications*, vol. 102, no. 5-6, pp. 515-522, Oct. 1993.
- [8] B. R. Frieden and A. T. Bajkova, "Bayesian cross-entropy reconstruction of complex images," *Applied Optics*, vol. 33, no. 2, pp. 219-226, Jan. 1994.
- [9] B. Borden, "Regularization of noisy ISAR images containing extended features," *IEEE Trans. Image Processing*, vol. 8, no. 1, pp. 124-127, Jan. 1999.
- [10] C. R. Vogel and M. E. Oman, "Fast, robust total variation-based reconstruction of noisy, blurred images," *IEEE Trans. Image Processing*, vol. 7, no. 6, pp. 813-824, June 1998.
- [11] P. Charbonnier, L. Blanc-Féraud, G. Aubert, and M. Barlaud, "Deterministic edge-preserving regularization in computed imaging," *IEEE Trans. Image Processing*, vol. 6, no. 2, pp. 298-310, February 1997.
- [12] D. C. Munson Jr., J. D. O'Brien, and W. K. Jenkins, "A tomographic formulation of spotlight-mode synthetic aperture radar," *Proc. IEEE*, vol. 71, pp. 917-925, Aug. 1983.
- [13] M. Çetin and W. C. Karl, "A statistical tomographic approach to synthetic aperture radar image reconstruction," *Proceedings of the 1997 IEEE International Conference on Image Processing*, vol. 1, pp. 845-848, Oct. 1997.